Surface, bulk, and interface electronic properties of nonpolar InN

W. M. Linhart,[1] T. D. Veal,[1] P. D. C. King,[1,a)] G. Koblmüller,[2,3] C. S. Gallinat,[2] J. S. Speck,[2] and C. F. McConville[1,b)]
[1]*Department of Physics, University of Warwick, Coventry CV4 7AL, United Kingdom*
[2]*Department of Materials, University of California, Santa Barbara, California 93106, USA*
[3]*Walter Schottky Institut, Technische Universität München, Am Coulombwall 3, 85748 Garching, Germany*

(Received 24 June 2010; accepted 22 August 2010; published online 13 September 2010)

The electronic properties of *a*-plane and *m*-plane InN have been investigated by x-ray photoemission spectroscopy, infrared reflectivity, and surface space-charge calculations. Electron accumulation has been observed at the surface of nonpolar InN and the surface Fermi level has been found to be lower than previously observed on InN samples. A high electron density in the InN close to the interface with GaN was found in each nonpolar InN sample. © *2010 American Institute of Physics*. [doi:10.1063/1.3488821]

Indium nitride (InN) has been the subject of intense research in recent years, largely due to its potential application in optoelectronic devices such as high-efficiency solar cells, light emitting diodes, and high-frequency transistors.[1] Despite extensive studies of many physical properties of InN, there remain limitations for device applications due to an electron accumulation layer at the InN surface.[2,3] However, for some applications, such as gas sensors and terahertz emitters, the presence of an electron accumulation layer is potentially beneficial.[1] Electron accumulation has been observed at the clean surface of wurtzite In- and N-polar *c*-plane and nonpolar *a*-plane InN,[4] and additionally at the nonpolar *m*-plane surface of InN nanocolumns,[5,6] as well as at the surface of zinc-blende InN.[4] Segev and Van de Walle[7] suggested from first-principles calculations the absence of the electron accumulation layer at the reconstructed surface of *a*-plane $(11\bar{2}0)$ and *m*-plane $(1\bar{1}00)$ InN because of the absence of In adlayers. This lack of electron accumulation was demonstrated on *in situ* cleaved *a*-plane InN (Ref. 8) but not on as-grown surfaces.[4,5,8–10]

This letter reports high resolution x-ray photoemission spectroscopy (XPS) and infrared (IR) reflectivity of nonpolar InN samples grown under In-rich and N-rich conditions. Using these techniques the surface Fermi level has been found to be lower than previously observed on as grown InN films. High values of the plasma frequency close to the interface with the GaN buffer layer have been found, indicating a high electron concentration in this region.

Nonpolar InN thin films were grown under either In- or N-rich conditions by plasma assisted molecular beam epitaxy. The *a*-plane $(11\bar{2}0)$ and *m*-plane $(1\bar{1}00)$ InN films were grown on *a*-plane and *m*-plane free-standing GaN (Mitsubishi Chemical Co.), respectively, with a ~50 nm (~20 nm) GaN buffer layer grown under Ga-rich conditions for *a*-plane (*m*-plane) InN.[11,12] Sample preparation was achieved by etching in a 10 mol/l HCl solution for 60 s to reduce the oxide layer. High-resolution XPS measurements were performed on samples of nonpolar InN using a Scienta ESCA300 spectrometer at the National Centre for Electron Spectroscopy and Surface analysis, Daresbury Laboratory, U.K. Details of the spectrometer are reported elsewhere.[13] The IR reflection from nonpolar InN samples was measured using a Bruker Vertex 70v Fourier transform IR spectrometer (FTIR). The reflection spectra were recorded for an incident and reflected angle of 35° to the surface normal. All measurements were performed at room temperature.

IR reflectivity was performed on the nonpolar InN films to determine their bulk conduction electron plasma frequency from which the bulk Fermi level (E_{bF}) position was found. The experimental and simulated IR reflectivity spectra are presented in Fig. 1. The oscillations observed in the experimental spectra are due to Fabry–Pérot interference, corresponding to the total InN film thickness (d_1+d_2, see Fig. 1). Each IR reflection spectrum was simulated using a two-

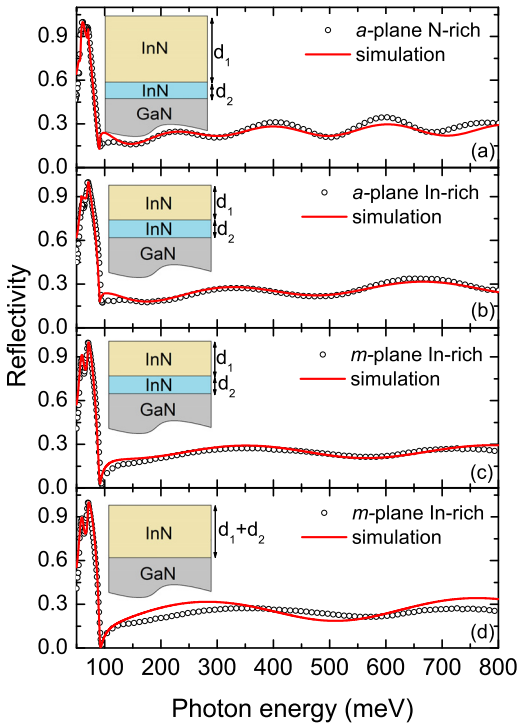

FIG. 1. (Color online) Experimental IR reflectivity spectra for nonpolar InN plotted with the simulated spectra. [(a)–(c)] The three layer model simulations. (d) A two layer model simulation. The insets show the layer models used in IR reflectivity simulations. In (d), the InN parameters determined for the bulk region in (c) have been used. Further adjustment of these parameters did not result in better agreement with the measured spectrum. The layer thicknesses (d_1 and d_2) are given in Table I.

a)Present address: School of Physics and Astronomy, University of St. Andrews, St Andrews, Fife KY16 9SS, United Kingdom.
b)Electronic mail: c.f.mcconville@warwick.ac.uk.

TABLE I. Parameters used in the IR reflectivity simulations, where ω_{TO}, ω_P, τ, and d are the longitudinal optical phonon frequency, the plasma frequency, the free-carrier lifetime, and layer thickness, respectively.

Sample	ω_{TO} (meV)	ω_P (meV)	τ (ps)	d (nm)
InN *a*-plane N-rich	58.2	84 ± 6	0.033 ± 0.004	950 ± 10
InN interface layer	58.2	300 ± 10	0.010 ± 0.003	80 ± 10
GaN	70.4	⋯	⋯	⋯
InN *a*-plane In-rich	58.2	85 ± 4	0.075 ± 0.008	510 ± 10
InN interface layer	58.2	290 ± 10	0.010 ± 0.003	70 ± 5
GaN	70.4	⋯	⋯	⋯
InN *m*-plane In-rich	58.2	60 ± 10	0.064 ± 0.030	410 ± 15
InN interface layer	58.2	290 ± 20	0.011 ± 0.003	60 ± 10
GaN	70.4	⋯	⋯	⋯

oscillator dielectric model. To account for the effects of surface roughness, partial coherency of the reflection was applied in the modeling but it had only a very small effect. Atomic force microscopy (AFM) was used to determine the morphology of the surface and the roughness of all nonpolar InN samples. The average roughness for *a*-plane and *m*-plane InN samples was 0.9 nm and 1.1 nm from the 3×3 μm^2 scans, respectively, and these values were used in the simulations. A three layer model consisting of an InN layer, an InN interface layer and bulk GaN was applied to simulate the experimental spectra [Figs. 1(a)–1(c)]. The high frequency dielectric constant and static dielectric constant for InN (InN interface layer, GaN), $\varepsilon(\infty)=7.80$ (Ref. 14) (6.90, 5.35) and $\varepsilon(0)=14.11$ (12.48, 8.90) have been used to simulate the IR reflectivity spectra. The other parameters used in the simulations are given in Table I. From the plasma frequency, the bulk carrier concentration has been calculated to be $1-2\times10^{18}$ cm^{-3}, and the bulk Fermi level position was found to be ~0.70–0.75 eV above the valence band maximum (VBM) for each nonpolar sample.

The VB photoemission for nonpolar InN and for previously studied *c*-plane InN (Ref. 15) is shown in Fig. 2. The position of the surface Fermi level (E_{sF}) was determined by extrapolating a linear fit to the leading edge of the VB

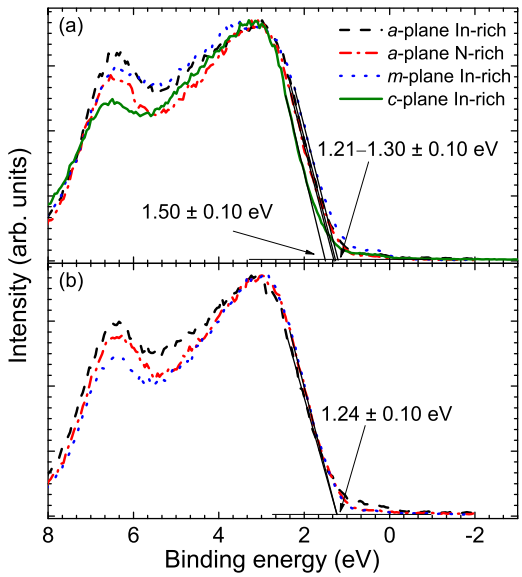

FIG. 2. (Color online) Valence band photoemission of the nonpolar InN and *c*-plane InN grown under In-rich conditions (solid line). (a) Spectra for as-loaded samples. (b) Spectra for cleaned samples.

TABLE II. Values of the surface Fermi level E_{sF} above the VBM from XPS measurements and bulk Fermi level E_{bF} above the VBM calculated using Fermi–Dirac carrier statistics. The band bending V_{bb} is calculated from the relative surface and bulk Fermi level positions. The bulk carrier concentration is determined from the plasma frequency using a nonparabolic band structure approximation (Ref. 21). Poisson-MTFA calculations give the surface state density n_{ss}.

InN	E_{sF} (eV)	E_{bF} (eV)	V_{bb} (eV)	n_b ($\times10^{18}$ cm^{-3})	n_{ss} ($\times10^{12}$ cm^{-2})
a-plane N-rich	1.24	0.75	0.49	2.3	9.9
a-plane In-rich	1.24	0.75	0.49	2.3	9.9
m-plane In-rich	1.24	0.71	0.53	1.2	9.7

photoemission.[16] It has been found that the E_{sF} for all nonpolar cleaned samples is 1.24 ± 0.10 eV. The values of E_{sF} are lower than previously determined for *c*-plane and *a*-plane InN.[4,10] Segev and Van de Walle suggested that the microscopic origin of donor-type surface states is In–In bonding in In adlayers at the InN surface.[7,17,18] This is consistent with core-level XPS measurements of the samples studied here, which indicate an In-rich surface in each case. Model calculations (using the scheme introduced in Refs. 13 and 19), indicate ~1 ML of In above the nonpolar InN bulklike termination in each case, significantly lower than found in a previous study of both *a*- and *c*-plane InN (3.0 ML and 3.4 ML, respectively).[13,19] One should note, however, that some residual oxygen contamination remained following the surface preparation, and one sample (*a*-plane In-rich InN) exhibited some In-droplets, observed by AFM, making detailed quantitative analysis of the adlayer coverage difficult.

Given a band gap of 0.64 eV,[20] the surface Fermi level is above the bottom of the conduction band, indicating a downward band bending at the surface of all the nonpolar InN samples. The E_{sF} and band bending values are listed in Table II. The surface state densities were determined by solving Poisson's equation within the modified Thomas–Fermi approximation (MTFA). Details of the calculations are reported elsewhere.[21] Figure 3 shows the band bending and carrier concentration profile for *m*-plane InN and *c*-plane InN. From Poisson's equation, the surface sheet density can be calculated from the gradient of the band bending potential at the surface. The surface sheet density n_{ss} for nonpolar InN films is $\sim9.9\times10^{12}$ cm^{-2} and for *c*-plane InN sample is $\sim14.0\times10^{12}$ cm^{-2}. The electron accumulation for *m*-plane InN has

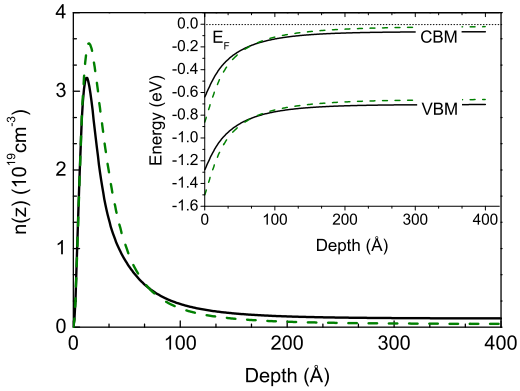

FIG. 3. (Color online) Carrier concentration as a function of depth from the surface for *m*-plane In-rich InN (solid line) and *c*-plane In-rich InN (dashed line). Inset: the conduction band minimum (CBM) and VBM positions with respect to the Fermi level, E_F, as a function of depth from the surface.

been found to be lower than for the *c*-plane InN film (Fig. 3). Whether these nonpolar samples exhibit the lowest achievable surface Fermi level for InN is not yet clear. More research involving the correlation of the surface electronic properties of InN with detail surface structural characterization is required, after different surface preparations. This would verify whether there is a causal link between the presence of In adlayers and surface electron accumulation and determine whether the latter can be further decreased.

As mentioned above, a three layer model has been applied in the modeling of the IR reflectivity spectra. A model containing just an InN layer and bulk GaN did not produce satisfactory simulated spectra, as shown in Fig. 1(d). Including a surface layer did not make much difference to the simulated spectra, in agreement with previous investigations,[22] and simulations with a graded interface[23] also made negligible difference. The plasma frequencies have been found to be 230–320 meV, corresponding to a sheet carrier concentration of $2.4-3.5\times10^{14}$ cm^{-2} for the interface layer. This is higher than previously determined for *c*-plane InN.[15] Several independent groups have discussed the origin of increased electron concentration close to the interface in *c*-plane InN by considering the possible effects of both unintentionally incorporated impurities and threading dislocation densities on the electron transport properties of InN.[23–28] The lower growth temperatures used for the growth of nonpolar InN [380–450 °C (Refs. 11 and 12)] compared with *c*-plane InN [450–540 °C (Refs. 27 and 29)] are likely to increase the impurity incorporation, increasing the density of donors close to the interface resulting in high plasma frequency values. This was confirmed by secondary ion mass spectrometry indicating that for *m*-plane InN the oxygen impurity density was approximately constant at 1×10^{17} cm^{-3} in the bulk InN and increased to 1×10^{18} cm^{-3} toward the InN/GaN interface, and then rapidly decreased to 5×10^{16} cm^{-3} in the bulk GaN. Moreover, Koblmüller *et al.*[11,12] have studied the structural properties of nonpolar InN and found basal-plane stacking faults where defects and/or impurities could be localized, contributing to the interface-related carrier concentration.

In conclusion, we have shown that the film quality of both *a*-plane and *m*-plane InN is significantly improved, as indicated by their lower bulk carrier concentration than many previous nonpolar InN films.[30] A high carrier concentration has been found in the nonpolar InN close to the interface with the GaN buffer layer, that may be due to donors associated with unintentionally incorporated impurities potentially localized at basal-plane stacking faults. The surface Fermi level for all nonpolar InN samples has been found to be lower than previously observed on noncleaved InN samples. The observation of an electron accumulation layer in the presence of a single In adlayer is consistent with previous theoretical predictions.

The work at Warwick was supported by RAINBOW, a Marie Curie Initial Training Network funded by the European Commission under the Seventh Framework program, Grant Agreement No. PITN-GA-2008-213238 and the Engineering and Physical Sciences Research Council, U.K., under Grant No. EP/G004447/1. We are grateful to D. Law of NCESS for his assistance with XPS measurements. The FTIR equipment used for this research was obtained, through Birmingham Science City: Creating and Characterizing Next Generation Advanced Materials, with support from Advantage West Midlands (AWM) and part funded by the European Regional Development Fund (ERDF). Work at UCSB was supported by AFOSR (Dr. Kitt Reinhardt, Program Manager) and made use of the Central Facilities supported by the NSF MRSEC Program under Grant No. DMR05-20415.

[1] *Indium Nitride and Related Alloys*, edited by T. D. Veal, C. F. McConville, and W. J. Shaff (CRC, Boca Raton, FL, 2009).
[2] H. Lu, W. J. Schaff, L. F. Eastman, and C. E. Stutz, Appl. Phys. Lett. **82**, 1736 (2003).
[3] I. Mahboob, T. D. Veal, C. F. McConville, H. Lu, and W. J. Schaff, Phys. Rev. Lett. **92**, 036804 (2004).
[4] P. D. C. King, T. D. Veal, C. F. McConville, F. Fuchs, J. Furthmüller, F. Bechstedt, P. Schley, R. Goldhahn, J. Schörmann, D. J. As, K. Lischka, D. Muto, H. Naoi, Y. Nanishi, H. Lu, and W. J. Schaff, Appl. Phys. Lett. **91**, 092101 (2007).
[5] E. Calleja, J. Grandal, M. A. Sánchez-García, M. Niebelschütz, V. Cimalla, and O. Ambacher, Appl. Phys. Lett. **90**, 262110 (2007).
[6] S. Lazić, E. Gallardo, J. M. Calleja, F. Agulló-Rueda, J. Grandal, M. A. Sánchez-Garcia, E. Calleja, E. Luna, and A. Trampert, Phys. Rev. B **76**, 205319 (2007).
[7] D. Segev and C. G. Van de Walle, Europhys. Lett. **76**, 305 (2006).
[8] C.-L. Wu, H.-M. Lee, C.-T. Kuo, C.-H. Chen, and S. Gwo, Phys. Rev. Lett. **101**, 106803 (2008).
[9] H. Lu, W. J. Schaff, L. F. Eastman, J. Wu, W. Walukiewicz, V. Cimalla, and O. Ambacher, Appl. Phys. Lett. **83**, 1136 (2003).
[10] T. Nagata, G. Koblmüller, O. Bierwagen, C. S. Gallinat, and J. S. Speck, Appl. Phys. Lett. **95**, 132104 (2009).
[11] G. Koblmüller, A. Hirai, F. Wu, C. S. Gallinat, G. D. Metcalfe, H. Shen, M. Wraback, and J. S. Speck, Appl. Phys. Lett. **93**, 171902 (2008).
[12] G. Koblmüller, G. D. Metcalfe, M. Wraback, F. Wu, C. S. Gallinat, and J. S. Speck, Appl. Phys. Lett. **94**, 091905 (2009).
[13] T. D. Veal, P. D. C. King, M. Walker, C. F. McConville, H. Lu, and W. J. Schaff, Physica B **401–402**, 351 (2007).
[14] R. Goldhahn, P. Schley, and M. Röppischer, in *Indium Nitride and Related Alloys*, edited by T. D. Veal, C. F. McConville, and W. J. Shaff (CRC, Boca Raton, FL, 2009), p. 336.
[15] P. D. C. King, T. D. Veal, C. S. Gallinat, G. Koblmüller, L. R. Bailey, J. S. Speck, and C. F. McConville, J. Appl. Phys. **104**, 103703 (2008).
[16] S. A. Chambers, T. Droubay, T. C. Kaspar, and M. Gutowski, J. Vac. Sci. Technol. B **22**, 2205 (2004).
[17] C. G. Van de Walle and D. Segev, J. Appl. Phys. **101**, 081704 (2007).
[18] D. Segev and C. G. Van de Walle, J. Cryst. Growth **300**, 199 (2007).
[19] T. D. Veal, P. D. C. King, P. H. Jefferson, L. F. J. Piper, C. F. McConville, H. Lu, W. J. Shaff, P. A. Anderson, S. M. Durbin, D. Muto, H. Naoi, and Y. Nanishi, Phys. Rev. B **76**, 075313 (2007).
[20] J. Wu, W. Walukiewicz, W. Shan, K. M. Yu, J. W. Ager III, S. X. Li, E. E. Haller, H. Lu, and W. J. Schaff, J. Appl. Phys. **94**, 4457 (2003).
[21] P. D. C. King, T. D. Veal, and C. F. McConville, Phys. Rev. B **77**, 125305 (2008).
[22] Y. Ishitani, X. Wang, S.-B. Che, and A. Yoshikawa, J. Appl. Phys. **103**, 053515 (2008).
[23] P. D. C. King, T. D. Veal, and C. F. McConville, J. Phys.: Condens. Matter **21**, 174201 (2009).
[24] C. Stampfl, C. G. Van de Walle, D. Vogel, P. Krüger, and J. Pollmann, Phys. Rev. B **61**, R7846 (2000).
[25] L. F. J. Piper, T. D. Veal, C. F. McConville, H. Lu, and W. J. Schaff, Appl. Phys. Lett. **88**, 252109 (2006).
[26] V. Lebedev, V. Cimalla, T. Baumann, O. Ambacher, F. M. Morales, J. G. Lozano, and D. González, J. Appl. Phys. **100**, 094903 (2006).
[27] C. S. Gallinat, G. Koblmüller, J. S. Brown, S. Bernardis, J. S. Speck, G. D. Chern, E. D. Readinger, H. Shen, and M. Wraback, Appl. Phys. Lett. **89**, 032109 (2006).
[28] X. Wang, S.-B. Che, Y. Ishitani, and A. Yoshikawa, Appl. Phys. Lett. **90**, 151901 (2007).
[29] G. Koblmüller, C. S. Gallinat, S. Bernardis, J. S. Speck, G. D. Chern, E. D. Readinger, H. Shen, and M. Wraback, Appl. Phys. Lett. **89**, 071902 (2006).
[30] V. Darakchieva, M. Schubert, T. Hofmann, B. Monemar, C.-L. Hsiao, T.-W. Liu, L.-C. Chen, W. J. Schaff, Y. Takagi, and Y. Nanishi, Appl. Phys. Lett. **95**, 202103 (2009).